

In situ energy dispersive x-ray reflectometry measurements on organic solar cells upon working

B. Paci,^{a)} A. Generosi, V. Rossi Albertini, and P. Perfetti

Istituto di Struttura della Materia-Area di Ricerca di Tor Vergata, Via del Fosso del Cavaliere 100, 00133 Roma, Italy

R. de Bettignies, M. Firon, J. Leroy, and C. Sentein

Commissariat à l'Energie Atomique, CEA Saclay, DRT-LITEN-DSEN-GENEC-L2C, F91191 Gif-sur-Yvette, France

(Received 24 May 2005; accepted 13 September 2005; published online 2 November 2005)

The change in the morphology of plastic solar cells was studied by means of time-resolved energy dispersive x-ray reflectivity (XRR). This unconventional application of the XRR technique allowed the follow up of *in situ* morphological evolution of an organic photovoltaic device upon working. The study consisted of three steps: A preliminary set of XRR measurements on various samples representing the intermediate stages of cell construction, which provided accurate data regarding the electronic densities of the different layers; the verification of the morphological stability of the device under ambient condition; a real-time collection of XRR patterns, both in the dark and during 15 h in artificial light conditions which allowed the changes in the system morphology at the electrode-active layer interface to be monitored. In this way, a progressive thickening of this interface, responsible for a reduction in the performances of the device, was observed directly.

© 2005 American Institute of Physics. [DOI: 10.1063/1.2128069]

In the engineering of plastic photovoltaic (PV) devices,^{1,2} several requirements must be fulfilled both in the choice of the materials and in the technology adopted. The materials used need to be intrinsically stable, characterized by high glass transition temperatures, and structurally resistant to cooling or heating. Furthermore, efficient purification methods, a water- and oxygen-free fabrication technique, and encapsulation of the structures after production are necessary conditions in cell construction.

A crucial problem to overcome in organic PV cell technology is device degradation.^{3,4} First, it is important to increase the device efficiency, this is because heating due to unconverted light can eventually damage the cells. Second, the devices need to be stable under storage conditions, while exposed to sunlight and under reduction or oxidation conditions. The main degradation agents, as reported in the literature, may have photochemical,^{5,6} electrochemical,⁷ or structural⁸ origins. Of particular concern is the fact that electrodes may react with the organic layer molecules: Metal diffusion from indium tin oxide (ITO) into polymers may occur [as has been observed in organic light emitting diodes of similar architecture]⁹ and photooxidation with oxygen at the interface electrode polymer can also be induced by illumination.

In recent years, using a variety of methods, several authors have studied various types of organic solar cells.¹⁰⁻¹² Nevertheless, the measurements were focused on electrical properties, efficiency and the response of the devices,^{2,13} while the structural and morphological changes accompanying the exposure to sunlight have not been accurately investigated.¹⁴ Therefore, the possibility of monitoring the changes experienced by the morphological parameters (thicknesses and roughness) *in situ* at the electrode-organic

layer interface, very sensitive to the possible reaction or diffusion processes involving the two materials, appears to be extremely useful. This would be an important step toward the detection of undesirable aging effects, which limit the present applications of the device, and it would give, as feedback, useful indications for exploring the architecture of new cell.

The XRR technique, commonly used to probe the properties of surfaces and interfaces of layered samples (films deposited on substrates, multilayers, superlattices etc.),¹⁵ is based on the Snell rule applied to x-rays.¹⁶ In the energy dispersive mode a polychromatic primary x-ray beam is used and the reflection patterns are collected at a fixed angle, by an ED solid-state detector.^{17,18} The use of EDXRR *in situ* prevents the problem of possible systematic errors in the removal and repositioning of the sample and allows the time evolution of the film morphology to be followed with extreme accuracy.¹⁹⁻²¹

The bulk heterojunction solar cells used in this study were made from methano-fullerene[6, 6]-phenyl C₆₁-butyric acid methyl ester, denoted as PCBM, and MDMO-PPV.

A ratio of 1:4 for MDMO-PPV:PCBM was used for the realization of the active layer, which had a thickness of 80 nm. The cells consisted of an ITO substrate cleaned in an ultrasonic bath with acetone and isopropanol, and oven dried. The active layer of MDMO-PPV:PCBM was deposited by spincoating from a chlorobenzene solution and the devices were completed by deposition of an aluminium layer (with a nominal thickness of 110 nm) through a shadow mask with 6 mm diameter openings. The active surface of these devices is 0.32 cm². Realization and initial electrical characterization of the cell were done under controlled atmospheric conditions (Fig. 1).

The EDXRR measurements were performed using a noncommercial laboratory energy dispersive x-ray reflectometer.¹⁷ The white incident beam is produced by a standard 2 kW tungsten anode x-ray tube and detection is

^{a)} Author to whom correspondence should be addressed; electronic mail: paci@ism.cnr.it

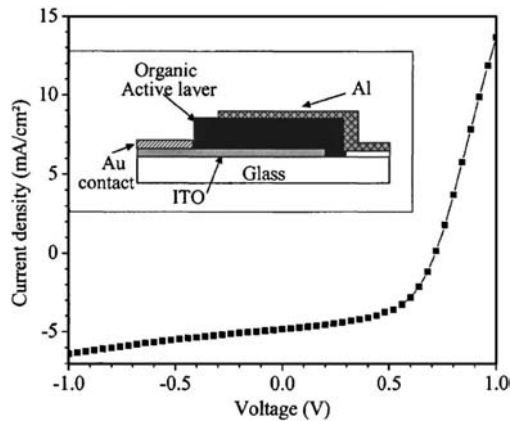


FIG. 1. The J/V characteristics under simulated AM1.5, 100 mW/cm² illumination of the bulk heterojunction device. The cell configuration is given in the inset. The PV parameters are $V_{oc}=0.715$ V, $J_{sc}=4.9$ mA/cm², FF=0.54, and $\eta=1.85\%$.

accomplished by a EG&G high-purity germanium solid-state detector. The energy resolution $\Delta E/E$ is $\sim 1.5\%$ in the energy range of interest (20–50 keV). Neither monochromator nor goniometer are required in the ED mode.

The cell under measurement was placed in an x-ray transparent chamber under controlled atmospheric conditions of N₂ gas flux to prevent contact with external oxidation agents, to be measured by EDXRR. The experimental approach consisted of a three-stage investigation. First, precursory *ex situ* XRR measurements were performed on the intermediate stages of cell construction in order to determine the electronic densities of the different layers. The morphological stability of the device under ambient conditions, when stored in the dark, was then verified, repeating the EDXRR *ex situ* measurements at different times (initially two sets of standard measurement). Finally, an *in situ* experiment, consisting of collecting a series of XRR spectra, each acquired for 30 min, over a total observation time of about 16 h was performed (third set of measurement).

In the case of a multilayered sample, the total XRR patterns are formed by the superposition of the signals coming from the various layers. Therefore, preliminary x-ray reflectivity measurements on three different samples, corresponding to successive stages of the cell construction, were carried out to identify the contributions of each layer to the overall cell reflection patterns (first set of measurement) separately (Fig. 2). The electronic densities obtained in this way will be used as fixed parameters in the Parrat formula²² utilized to fit the data.

Before proceeding with the *in situ* experiment, the stability of the device, under ambient condition was verified by *ex situ* EDXRR measurements (second set of measurement, performed keeping the cell in the dark). The inset of Fig. 3 shows that no change in the spectra is visible, even repeating the measurement after some months, which demonstrates that the cell morphology is stable for long times if the cell is not illuminated.

The results of the *in situ* EDXRR measurements on a solar cell, performed under controlled atmospheric conditions and, upon illumination, are reported in Fig. 3 (third set of measurements). The two initial patterns were collected keeping the cell in the dark (first hour) and, then, a sequence of 30 patterns were collected during the illumination of the

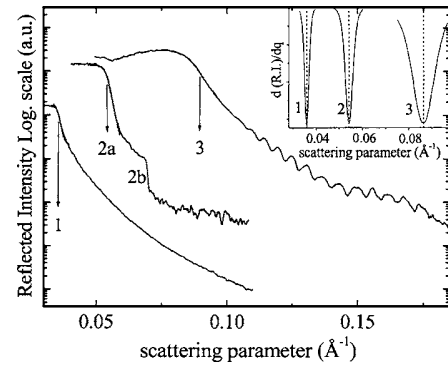


FIG. 2. The XRR measurements performed on three different samples, corresponding to subsequent stages of the cell construction: (1) Glass/ITO/MDMO-PPV+PCBM, (2) glass/ITO, and (3) glass/ITO/MDMO-PPV+PCBM/Al. The accurate determination of the critical edge of the EDXRR patterns, via the fit of the reflection curve ($R.I.$) derivative, allows us to calculate the electronic densities of the various layers: (1) Organic film $\rho=8.5 \times 10^{-5} \text{ \AA}^{-2}$; (2) ITO electrode $\rho=2.06 \times 10^{-4} \text{ \AA}^{-2}$; and (3) Al electrode $\rho=5.35 \times 10^{-4} \text{ \AA}^{-2}$. The intensity drop-off indicated as (b) is the In adsorption edge.

cell by a white lamp (10 mW/cm²) for the subsequent 15 h.

The reflectivity profiles are shifted in height for clarity. Each reflectivity curve is quite complicated, being the result of the different contributions of the various layers and, at high q values, small angle scattering from the glass is also present. The oscillations visible between 0.010 \AA^{-1} and 0.013 \AA^{-1} are due to the Al film and the fit of the data, according to Parrat model,²² allows its thickness to be determined. Since the film thickness is proportional to the number of oscillations present in the observed q range of the EDXRR pattern, its determination is not limited by the spectral resolution, which influences the oscillation shape (broadening the sharp features) but not their wavelength.

The first two curves (bottom curves in Fig. 3), collected before the illumination of the cell was initiated, are identical, while as the cell is illuminated, a change in the EDXRR profiles is visible: The slight change in the period of the

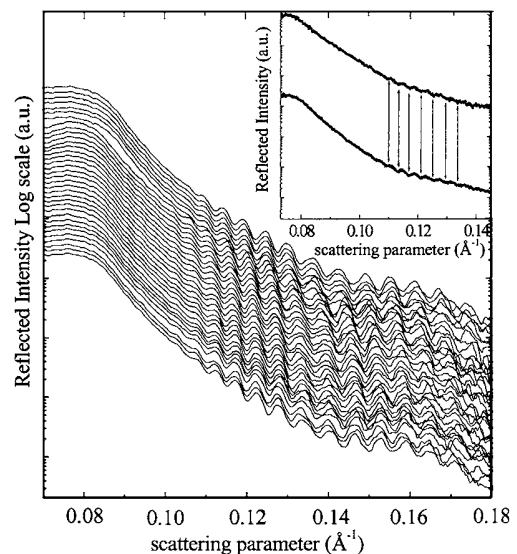


FIG. 3. *In situ* EDXRR measurements of the solar cell, collected under controlled atmosphere and upon illumination. The reflectivity profiles are shifted in height for clarity. Inset: the *ex situ* EDXRR measurements carried out at a distance of several months on the same cell.

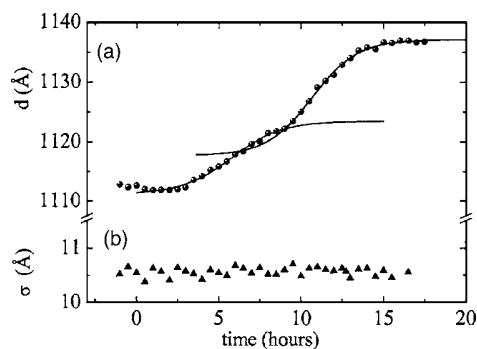


FIG. 4. Al film thickness $d(t)$ and roughness $\sigma(t)$ as a function of time, obtained by fitting the spectra of Fig. 3 using Parrat's model (Ref. 22). The solid lines represent the fit of the data points according to two independent Boltzman growth functions, $x(t) = x_1 + (x_2 - x_1) (1 - \exp(-t/\tau))$. The amplitude and time constant of the first process are $\Delta x = 10 \text{ \AA}$ and $\tau = 6 \text{ h}$. The second process is activated when the first one is almost concluded ($\Delta x = 20 \text{ \AA}$, $\tau = 11 \text{ h}$).

oscillations is related to the increase in Al film thickness d .^{23–25} The characteristic feature of the EDXRR sequence is a continuous shift of the minima (of the oscillations between 0.010 \AA^{-1} and 0.013 \AA^{-1}) toward lower q values, which is visible even by the naked eye. Since the Al film thickness d is connected to the oscillation period of the curves in Fig. 3 (Δq) by the approximate relation $d = 2\pi/\Delta q$, this shift witnesses the increase of d as a consequence of the exposure to light. This observation assures that no artifact can be introduced by the fit procedure. Indeed, the general characteristics of the $d(t)$ curve are known *a priori* and the fit result must be in agreement with them.

Two possible explanations can be given for the electrode thickening. One is that the Al film growth is due to the formation of an aluminium oxide layer at the film surface and at its interface with the organic film consequent to a photo-oxidation reaction. In this case, the thickening is a “real” effect. Alternatively, the increase in the metal electrode thickness could be “apparent” and might be produced by the formation of a layer at the Al-organic film interface due to indium diffusion from the ITO.⁹ Indeed, in the latter case, since the electronic scattering length density of the resulting layer is very close to that of pure Al, the change in the EDXRR signal would be indistinguishable from that due to a thickening of the Al film.²³

The changes in the two morphological parameters are quantified in more rigorous terms by analyzing all the reflection patterns acquired. The thickness and roughness (σ) versus time curve is plotted in Fig. 4. As expected, the Al film thickness increases upon illumination of the cell, from an initial value of 1111 \AA to a final value of approximately 1137 \AA (exact values as measured by EDXRR, the original Al layer being slightly thicker than the nominal one).

The σ versus t curve is plotted in Fig. 4(b), showing that the parameter remains almost unchanged [$10.5(5) \text{ \AA}$]. This may indicate either that the observed process is limited to the interface between the Al and the organic film, or that the thickening process proceeds smoothly (as expected in the hypothesis of an oxidation process).

A last comment regarding the actual shape of the d versus t curve. In Fig. 4, the high statistical accuracy of the data allow us to reveal a more complex behavior not fully reproduced by a simple Boltzman sigmoidal curve, $x(t) = x_1 + (x_2$

$-x_1)[1 - \exp(-t/\tau)]$, which describes the case of the progressive increase of a given parameter x , from its initial value x_1 up to its asymptotical value x_2 (saturation), in a characteristic time τ . In the present case, $x(t)$ represents the evolution over time of the film thickness as obtained from the curves in Figs. 4(a). The modulation in the $d(t)$ plot suggests that two independent photoinduced phenomena are occurring, with different characteristic times. Therefore, two Boltzman sigmoidal curves were used in the fit. It can be noticed that the first process is almost concluded when the second starts to be activated.

In summary, the morphology of the PV device is shown to be stable upon storage in the dark. On the contrary, an increase of the Al electrode thickness is visible upon illumination: After an increase of about 30 \AA , the thickening process is concluded in 13 h. Furthermore, the high statistical accuracy of the time-resolved EDXRR data allowed us to detect a two-step modulation in the curve describing the Al film thickening process. Therefore, the results reported demonstrate that the EDXRR technique applied *in situ* is a powerful nondestructive tool to investigate the aging effects at the interface of polymer PV cells in working conditions.

The authors are grateful to A. Casling for his critical reading of the manuscript.

¹N. S. Sariciftci, L. Smilowitz, A. J. Heeger, and F. Wudl, *Science* **258**, 1474 (1992).

²C. J. Brabec, S. E. Shaheen, C. Winder, N. S. Sariciftci, and P. Denk, *Appl. Phys. Lett.* **80**, 1288 (2002).

³F. Padinger, R. S. Rittberger, and N. S. Sariciftci, *Adv. Funct. Mater.* **13**, 85 (2003).

⁴T. Jeranko, H. Tributsch, N. S. Sariciftci, and J. C. Hummelen, *Sol. Energy Mater. Sol. Cells* **83**, 247 (2004).

⁵J. Turro, *Modern Molecular Photochemistry* (University Science, Mill Valley, CA, 1991).

⁶H. Neugebauer, C. Brabec, J. C. Hummelen, and N. S. Sariciftci, *Sol. Energy Mater. Sol. Cells* **61**, 35 (2000).

⁷M. Yahiro, D. Zou, and T. Tsutsui, *Synth. Met.* **245**, 111 (2000).

⁸J. M. Kroon, M. M. Wien, W. J. H. Verhees, and J. C. Hummelen, *Thin Solid Films* **223**, 403 (2002).

⁹E. Gautier, A. Lorin, J. M. Nunzi, A. Schalchli, J. J. Benattar, and D. Vital, *Appl. Phys. Lett.* **69**, 1071 (1996).

¹⁰W. U. Huynh, J. J. Dittmer, and A. P. Alvisatos, *Science* **295**, 2425 (2002).

¹¹P. K. H. Ho, J.-S. Kim, J. H. Burroughes, H. Becker, S. F. Y. Li, T. M. Brown, F. Cacialli, and R. H. Friend, *Letters to Nature* **404**, 481 (2000).

¹²J. M. Nunzi, *C. R. Phys.* **3**, 523 (2002).

¹³L. Sicot, C. Fiorini, A. Lorin, J.-M. Nunzi, P. Raimond, and C. Seintin, *Synth. Met.* **102**, 991 (1999).

¹⁴S. E. Shaheen, C. J. Brabec, N. S. Sariciftci, F. Padinger, T. Fromherz, and J. C. Hummelen, *Appl. Phys. Lett.* **78**, 841 (2001).

¹⁵X. L. Zhou and S. H. Chen, *Phys. Rep.* **257**, 226 (1995).

¹⁶R. W. James, *The Optical Principles of Diffraction of X-Ray* (Oxbox, Woodbridge, Connecticut, 1982).

¹⁷R. Caminiti and V. Rossi Albertini, *Int. Rev. Phys. Chem.* **18**, 263 (1999).

¹⁸K. Orita, T. Morimura, T. Horiuchi, and K. Matsushige, *Synth. Met.* **91**, 155 (1997).

¹⁹V. Rossi Albertini, A. Generosi, B. Paci, P. Perfetti, G. Rossi, A. Capobianchi, A. M. Paoletti, and R. Caminiti, *Appl. Phys. Lett.* **82**, 3868 (2003).

²⁰A. Generosi, B. Paci, V. Rossi Albertini, P. Perfetti, G. Pennesi, A. M. Paoletti, G. Rossi, A. Capobianchi, and R. Caminiti, *Appl. Phys. Lett.* **86**, 114106 (2005).

²¹J. C. Malaurent, H. Duval, J. P. Chauvineau, O. Hainaut, A. Raynal, and P. Dhez, *Opt. Commun.* **173**, 255 (2000).

²²L. G. Parrat, *Phys. Rev.* **95**, 359 (1954).

²³S. J. Roser, R. Felici, and A. Eaglesham, *Langmuir* **10**, 3853 (1994).

²⁴S. K. Sinha, E. B. Sirota, S. Garoff, and H. B. Stanley, *Phys. Rev. B* **38**, 2297 (1988).

²⁵A. Cotton and G. Wilkinson, *Advanced Inorganic Chemistry* (Wiley, New York, 1999).